# Predicting the Liquid Phase Mass Transfer Resistance of Structured Packings*

**Ž. Olujić[a,+] and A. F. Seibert[b]**

[a]Process & Energy Laboratory, Delft University of Technology, Leeghwaterstraat 39, 2628 CB Delft, The Netherlands

[b]Separations Research Program (SRP), The University of Texas at Austin, Austin, TX 78712, USA

doi: 10.15255/CABEQ.2014.19344

Review
Received: May 5, 2014
Accepted: November 25, 2014

Published correlations for estimating the liquid phase mass transfer coefficients of structured packings are compared using experimental evidence on the efficiency of Montz-Pak B1–250MN and B1–500MN structured packings as measured in total reflux distillation tests using the chlorobenzene/ethylbenzene system at two operating pressures. Large differences are found between different correlations with respect to both the absolute values of mass transfer coefficients and the fraction of liquid phase based resistance and their trends with respect to increasing vapor and liquid loads. A new Delft Model liquid side mass transfer coefficient correlation that incorporates a more appropriate definition of the liquid film exposure length is presented which now generates lower values. The revised liquid film model, combined with an enhanced turbulent vapor phase mass transfer coefficient, leads to doubling the fractional liquid phase resistance with respect to that based on penetration theory assuming equal contact times. This effect results in predicting efficiencies which are slightly more conservative and agree reasonably well with experimental HETP data presented in this paper.

*Key words:*
distillation, structured packings, mass transfer, liquid phase resistance

## Introduction

Refining, gas processing, and commodity chemicals manufacturing plants around the world are continuously looking for ways to reduce energy requirements because of the immense costs associated with operation of large scale distillation facilities. Recent advances in improving energy efficiency of distillation equipment are summarized in a review paper by Olujić et al.[1]

Thermodynamically, the energy efficiency of distillation columns tends to increase with decreasing pressure drop. Being characterized by the lowest pressure drop per equilibrium stage (theoretical plate), corrugated sheet structured packing is the preferred choice and widely used where appropriate, such as in vacuum and near atmospheric applications.

In the late 1990s, first generation packings were improved by modifying the macro-geometry of triangular flow channels.[2] The newer generation of high capacity corrugated sheet structured packings, with the lower and in some cases both ends of corrugations bent to vertical,[3,4] allows smooth transition of both phases and shifts the point of onset of loading to significantly higher vapor loads compared to conventional geometries. With higher throughputs and similar efficiency, the high capacity packings have been used to revamp existing columns. The motivation is usually the need to increase the profitability and not the sustainability of an existing plant. The latter could be realized if the efficiency of the established structured packings could be enhanced allowing operation closer to the minimum reflux ratio. To achieve improved efficiency, a better fundamental understanding of governing mass transfer phenomena must be acquired.

The operating principle of corrugated sheet structured packings is simple. It is basically a film flow device where the available packing surface area promotes actual vapor-liquid mass transfer area. Such packing requires that the entering liquid and vapor are evenly distributed so that the two phases will be permanently exposed to a dynamic contact across a maximum interfacial area with a maximum driving force. The rising vapor and falling liquid flow in a zigzag flow pattern imposed by the internal structure of the packed bed consisting of packing elements or layers rotated to each other

*Based on a paper presented at Distillation 2011: **The James R. Fair Heritage Distillation Conference**, AIChE Spring National Meeting, March 13–17, 2011, Chicago, Illinois, USA

+Corresponding author: z.olujic@tudelft.nl

by 90 degrees. The transitions between packing elements or layers can introduce flow discontinuities which are less pronounced in the new generation of high capacity packings with corrugation ends bent to vertical.

Liquid distributes accordingly with adequate initial irrigation density and within one or two packing layers, a thin liquid film spreads over the installed surface creating an exposed interface. According to predictive models, in the preloading region without pronounced interference of ascending vapor and descending liquid, interfacial or effective area tends to increase with increasing liquid load. Its relative magnitude however depends on many factors and cannot be determined with certainty. Tsai and coworkers have studied the effect of liquid and gas velocities on the effective contact area.[5] This paper focuses on mass transfer coefficients, with particular emphasis on the qualitative and quantitative modeling aspects of the liquid phase related mass transfer resistance.

## Previous Work

The interface is established at the surface of a moving liquid film which as a result of gravity flows downward at an angle steeper than the corrugation inclination angle. The effective velocities of both phases and exposure (contact) time depend mainly on the corrugation inclination angle and the liquid holdup which is generally low in the preloading region.

According to well established two-film theory, total resistance to mass transfer is described as a sum of individual vapor and liquid phase contributions. Since the vapor (gas) phase resistance typically dominates in distillation, it is a common practice to write the overall expressions based on the vapor side.[6] While this is generally accepted, the relative contribution of the liquid phase resistance is uncertain.

In a recent paper, Harriott[7] evaluated published correlations for the local efficiency of cross-flow distillation trays and found that these give widely different values of the liquid-phase resistance. He concluded that penetration theory reasonably describes the relationship between the operating pressure and the magnitude of the liquid resistance in distillation and for a typical binary mixture at atmospheric pressure when the equilibrium line slope is near unity, the liquid side contribution should not exceed 15 %.

The liquid phase contribution could be even less pronounced for corrugated sheet structured packing. Origins of this belief are difficult to trace but justification can be found in early studies conducted with a wetted wall falling film distillation column, (see, for example, Johnstone and Pigford[8]) indicating that not more than 10 % of total resistance to mass transfer lies in the liquid phase. However, this indication appears to be low when considering the results of theoretical and experimental studies conducted in mid and late 1970s by Sandall and co-workers.[9–11] Their theoretical and experimental effort has been arranged to allow direct determination of individual vapor and liquid phase mass transfer coefficients from falling film and packed column total reflux binary distillation studies. They arrived at the conclusion that the liquid phase resistance is small but not negligible and should range somewhere between 12 and 18 %.[11]

The liquid phase resistance in distillation is often considered practically negligible,[12] and this assumption is a common basis for development of short cut calculation methods.[13] However on occasion, there is evidence appearing in the open literature claiming the opposite, suggesting that the liquid phase resistance is not only significant but can exceed that of the vapor phase.[14,15] For instance, Chen and Chuang[14] have evaluated the results of total reflux distillation tests performed with six binary mixtures in a sieve tray column including aqueous and organic systems. They came to the conclusion that the liquid-phase resistance to mass transfer is significant ranging from 20 to 50 % and could reach higher values in cases where the equilibrium line slope is larger than one. They consider the general belief that the distillation is a vapor-controlled operation to be arbitrary and not reliable. Similar values are claimed by Rejl et al.[15] based on the evaluation of liquid and vapor phase concentration profiles measured along the packed bed during total reflux distillation tests carried out with binary mixtures of primary alcohols. These data have been used to validate established predictive models and it appeared that in conjunction with high values of the equilibrium line slope, the liquid phase fraction of the total resistance could exceed that of the vapor.

In this paper, published correlations for prediction of the liquid side mass transfer coefficient of structured packings are reviewed and compared. In addition, a modification of the Delft liquid phase film coefficient model is introduced that adopts a more realistic liquid contact length as a characteristic linear dimension.

## Modeling Considerations

### Working equations

The packed bed height, $h_{pb}$ (m), required to produce desired separation is defined as

$$h_{pb} = HTU_{Go} \cdot NTU_{Go} = HETP \cdot N \qquad (1)$$

where $HTU_{Go}$ (m) is the height of overall vapor phase transfer unit, $NTU_{Go}$ (–) is the number of overall vapor phase transfer units, *HETP* (m) is the height equivalent to a theoretical plate, and $N$ (–) the number of equilibrium stages or theoretical plates.

Packing manufacturers and users often rely on the *HETP* as the measure of packing efficiency since $N$ can usually be determined with ease using rigorous models available in various commercial process simulation software packages. While the *HETP* is basically an empirical quantity, it is directly related to theoretically founded height of transfer unit through the transformed and extended form of the expression (1), which is generally valid if the equilibrium and operating lines are straight.

$$HETP = \frac{NTU_{Go}}{N} HTU_{Go} = \frac{\ln \lambda}{\lambda - 1} HTU_{Go} = \\ = (HTU_G + \lambda HTU_L) \frac{\ln \lambda}{\lambda - 1} \tag{2}$$

where $HTU_G$ (m) and $HTU_L$ (m) represent the height of vapor and liquid phase transfer units. The magnitude of the liquid phase resistance contribution depends on the value of the stripping factor, $\lambda$ (–), the ratio of slopes of equilibrium and operating lines:

$$\lambda = \frac{m}{(L/G)} = \frac{mG}{L} = m \frac{u_{Gs} \rho_G M_{wL}}{u_{Ls} \rho_L M_{wG}} \tag{3}$$

where $G$ (kmol s$^{-1}$) and $L$ (kmol s$^{-1}$) are molar flow rates, $u_{Gs}$ (m s$^{-1}$) and $u_{Ls}$ (m s$^{-1}$) are superficial velocities, $\rho_G$ (kg m$^{-3}$) and $\rho_L$ (kg m$^{-3}$) are densities, and $M_{wG}$ (kg kmol$^{-1}$) and $M_{wL}$ (kg kmol$^{-1}$) are molar masses of vapor (gas) and liquid, respectively.

In the case of total reflux distillation ($L = G$, i.e. $u_{Gs}\rho_G M_{wG}^{-1} = u_{Ls}\rho_L M_{wL}^{-1}$), as usually employed for purposes of packing performance tests, the stripping factor becomes equal to the slope of the equilibrium line, i.e. $\lambda = m$ (-).

The local slope of the equilibrium line is a function of relative volatility, $\alpha$ (-) and the composition, i.e. the mole fraction of more volatile component, $x$ (-).

$$m = \frac{\mathrm{d}y}{\mathrm{d}x} = \frac{\alpha}{[1 + (\alpha - 1)x]^2} \tag{4}$$

This implies that the slope of the equilibrium line changes along the packed bed or column to the extent depending on the composition and relative volatility. According to Eq. (4), the dependence of $m$ on the composition increases with increasing $\alpha$. However, when $\alpha < 1.2$ (close boiling mixtures), the equilibrium line slope $m \approx 1$.

By substituting the overall and individual heights of the transfer unit using the corresponding ratios of superficial vapor velocity and the volumetric mass transfer coefficients, Eq. (2) becomes

$$HETP = \frac{u_{Gs}}{k_{Go} a_e} \frac{\ln m}{m - 1} = \left( \frac{u_{Gs}}{k_G a_e} + m \frac{u_{Ls}}{k_L a_e} \right) \frac{\ln m}{m - 1} = \\ = \frac{u_{Gs}}{k_G a_e} \left( 1 + m \frac{k_G}{k_L} \frac{u_{Ls}}{u_{Gs}} \right) \frac{\ln m}{m - 1} \tag{5}$$

where $k_{Go}$ (m s$^{-1}$) is overall vapor side based mass transfer coefficient, $a_e$ (m$^{-1}$) is effective or interfacial area, and $k_G$ (m s$^{-1}$) and $k_L$ (m s$^{-1}$) are mass transfer coefficients of vapor and liquid phase, respectively.

The expressions within parentheses of Eqs. (2) and (5) represent the overall resistance to mass transfer, which means that the fraction of the liquid side resistance, *LRF* (-), in case of total reflux can be expressed as

$$LRF = \frac{m\, HTU_L}{HTU_G + m\, HTU_L} = \\ = \frac{m \frac{k_G}{k_L} \frac{u_{Ls}}{u_{Gs}}}{1 + m \frac{k_G}{k_L} \frac{u_{Ls}}{u_{Gs}}} = \frac{m \frac{k_G}{k_L} \frac{\rho_G}{\rho_L}}{1 + m \frac{k_G}{k_L} \frac{\rho_G}{\rho_L}} \tag{6}$$

As shown in Eq. (6), the fraction of the liquid phase resistance increases as $m$, ($\rho_G/\rho_L$) and/or ($k_G/k_L$) increases. For the given test system, with $m = 1$, the density ratio tends to increase with increasing pressure suggesting that an increase in the operating pressure and/or pressure drop will lead to an increase in the fraction of liquid phase resistance, where the magnitude will depend on the value of the ratio of vapor and liquid mass phase mass transfer coefficients.

If penetration theory and equivalent contact times are assumed to be valid for both phases, then the ratio ($k_G/k_L$) reduces to the square root of the ratio of vapor to liquid phase diffusion coefficients[6], i.e. $(D_G/D_L)^{0.5}$. Therefore, the fraction of liquid phase resistance is independent of the contactor used and depends only on the physical properties of the system which will change with variations in pressure or temperature.

However, the assumption of equal contact time for both phases is valid only if the lifetime of the interface is identical with the residence time of the vapor in two-phase layer. According to Stichlmair and Fair,[6] this is very likely to be the case with the froth regime on a tray because the interface appears to be produced by penetration of the gas into the liquid. However, this is not the case with corrugated sheet

structured packing where, in the preloading region, the interface is a rather undisturbed surface of a liquid film that flows downward along an inclined wall driven by gravity. As shown in Table 1 for the liquid phase mass transfer coefficient, and from corresponding vapor phase correlations (see original references), the values of the exponent of the diffusion coefficient vary in both cases between 0.5 and 1. Unfortunately, the knowledge on how other factors influence the mass transfer rate on both sides of the interface is not well understood. As a consequence, the relative contribution of the two individual resistances may vary considerably depending on corresponding correlations within a model which must be used together to predict the overall mass transfer coefficient.

### Mass transfer coefficient correlations considered

A recent review of mass transfer models for structured packings, e.g. Wang et al.[16] includes correlations associated with nine models published from 1985 to 2005: Bravo et al.[17]; Nawrocki et al.[18]; de Britto et al.[19]; Hanley et al.[20]; Rocha et al.[21]; Brunazzi and Paglianti[22]; Shetty and Cerro[23]; Billet and Schultes[24]; Olujić et al.[25,26]; and Xu et al.[27]. The model introduced by Bravo, Rocha and Fair[17] was developed for gauze packing. After publication of the Wang et al.[16] paper, Del Carlo et al.[28] introduced a generalized correlation, which is similar to Brunazzi and Paglianti.[22] Most recently, Hanley and Chen[29] introduced new correlations that are used within the column performance simulation package ASPEN.

The seven models compared in this study are generally considered suitable for conventional metal sheet packings. These are, in alphabetic order: Billet and Schultes (B&S); Brunazzi and Paglianti (B&P), including Del Carlo, Olujić and Paglianti (dCOP); Delft Model (DM); Hanley and Chen (H&C); Nawrocki, Xu, and Chuang (NXC); Rocha, Bravo and Fair (RBF); and Shetty and Cerro (S&C). The abbreviated names are used in graphs and in the text for convenience.

The working equations of these models are shown in the order of appearance in Table 1. In order to be able to estimate the fraction of resistance caused by liquid phase, each liquid phase correlation considered in this study is used in combination with its corresponding vapor phase correlation. These are not listed in the present paper but can be found in their respective references.

## Base Case

The base case packing is a corrugated sheet metal structured packing with a specific geometric area of 250 $m^2$ $m^{-3}$. A packing with 500 $m^2$ $m^{-3}$ is also considered to illustrate the effect of specific geometric area. Some models require specific packing type and size related coefficients which are given in Table 1. Figure 1 shows relevant geometric dimensions of corrugated sheet structured packings. Characteristic values associated with two packing sizes considered in this study are shown in Table 2.

The operating conditions correspond to those encountered in total reflux distillation tests carried out with various Montz structured packings at Bayer TS using chlorobenzene/ethylbenzene (CB/EB) as the test system,[30] operated at 0.1 and 1 bar. A factor 10 difference in operating pressure allows the evaluation of a substantial change in relevant physical properties. The physical properties are summarized in Table 3 and represent an average corresponding to the middle of the bed conditions. The physical property estimation methods for this system are based on the publication of Ottenbacher et al.[31] which is considered the most accurate for CB/EB system according to industrial standards.

An advantage of the CB/EB test mixture is reflected in the fact that it is a close boiling system where the slope of the equilibrium line is essentially equal to one for both pressures. Therefore, possible composition and relative volatility related effects are eliminated from consideration.

## Results and Discussion

### Liquid phase mass transfer coefficient model prediction comparisons

Predicted liquid phase mass transfer coefficients using the different methods for the B1–250 packing at 0.1 bar are shown in Fig. 2a as a function of the vapor load expressed as F-factor. One should note that, under total reflux conditions, an increase in F-factor implies a proportional increase in the liquid load. All correlations exhibit an increasing $k_L$ trend with increasing F-factor. The DM method predicts highest values, followed by B&S and NXC (similar values), then B&P and dCOP models. The lowest values are predicted by S&C and H&C methods. The values predicted by Del Carlo et al. correlation[28] follow the same trend differing slightly from the original Brunazzi and Paglianti[22] correlation by a factor corresponding to the value of (sin $\alpha$), added in the former case in the expression of the Graetz number. Further considerations will include the original BP method only.

The difference between RBF and DM values is a result of the characteristic linear dimension; in the RBF case it is the corrugation side length ($s$), while the hydraulic diameter of the triangular vapor flow channel ($d_{hG}$) is used in the DM method. For a corrugated sheet structured packing with a 90° fold angle,

Table 1 – *Working equations of the liquid phase mass transfer models considered in this study*

**NXC** – Nawrocki, Xu, Chuang[18]

$$k_L = 2\sqrt{\frac{D_L}{\pi}\frac{u_{Le}}{s}} = 2\sqrt{\frac{D_L}{\pi}\frac{3u_{Ls}}{a_p 2\delta s}} \tag{7}$$

with

$$\delta = \left(\frac{3\,\mu_L}{\rho_L\, g\, a_p}\,\frac{u_{Ls}}{\sin\alpha}\right)^{1/3} \tag{7a}$$

**RBF** – Rocha, Bravo, Fair[21]

$$k_L = 2\sqrt{\frac{D_L}{\pi} C_e \frac{u_{Le}}{s}} = 2\sqrt{\frac{D_L}{\pi} C_e \frac{u_{Ls}}{\varepsilon\, h_L\, s\, \sin\alpha}} \tag{8}$$

with $C_e$ = 0.9 (in present study $C_E$ = 1).

**S&C** – Shetty, Cerro[23]

$$k_L = \frac{D_L}{b} 0.4185 \sqrt{\frac{\sin\alpha}{l_r}}\, \mathrm{Re}_L^{1/3}\, Ga_L^{1/6}\, Sc_L^{1/2} \tag{9}$$

with

$$\mathrm{Re}_L = \frac{u_{Ls}\rho_L}{a_p \mu_L}\ ;\ Ga_L = \frac{g\, b^3 \rho_L^2}{\mu_L^2}\ ;\ Sc_L = \frac{\mu_L}{D_L \rho_L}\ ; \quad \text{(9a; 9b; 9c)}$$

and

$$l_r = 3.7617 - 0.12299\alpha + 0.001976\alpha^2 - 1.1167\cdot 10^{-5}\alpha^3\,. \tag{9d}$$

**B&P** – Brunazzi, Paglianti[22]

$$k_L = \frac{D_L}{4\delta} 16.43 \cdot Gz_L^{0.915}\, Ka_L^{-0.09} \tag{10}$$

with

$$Ka_L = \frac{\sigma^3 \rho_L}{g\,\mu_L} \quad \text{and}$$

$$Gz_L = \mathrm{Re}_L\, Sc_L \left(\frac{\delta}{h_{pe}}\right) = \left(\frac{\rho_L u_{Ls} 4\delta}{\mu_L h_L \sin\alpha}\right)\left(\frac{\mu_L}{D_L \rho_L}\right)\left(\frac{\delta}{h_{pe}}\right) \quad \text{(10a, 10b)}$$

where

$$\delta = \left(\frac{3\,\mu_L}{\rho_L\, g \sin\alpha}\,\frac{u_{Ls}}{h_L \sin\alpha}\right)^{1/2} \tag{10c}$$

and

$$h_L = 0.0169 \cdot a_p^{0.37} \left(3600\, u_{Ls}\right)^{0.37} \left(\frac{\mu_L}{0.001}\right)^{0.25} \tag{10d}$$

**B&S** – Billet, Schultes[24]

$$k_L = C_L \cdot 12^{1/6} \cdot \sqrt{\frac{D_L\, u_{Ls}\, a_p}{4\varepsilon h_L}} \tag{11}$$

with

$$h_L = \left(12\,\frac{u_{Ls}\, a_p^2 \mu_L}{\rho_L\, g}\right)^{1/3} \tag{11a}$$

$C_L$ = 1.068 for B1–250, and $C_L$ = 1.54 for B1–500 packing, respectively.

**DM** – Delft Model[25,26]

$$h_L = 2\sqrt{\frac{D_L}{\pi}\frac{u_{Le}}{0.9 d_{hG}}} = 2\sqrt{\frac{D_L}{\pi}\frac{u_{Ls}}{0.9 d_{hG}\varepsilon h_L \sin\alpha_L}} \tag{12}$$

with

$$d_{hG} = \frac{2hb}{2s+b} \tag{12a}$$

$$\delta = \left(\frac{3\mu_L\, u_{Ls}}{\rho_L\, g\, a_p\, \sin\alpha_L}\right)^{\frac{1}{3}} \quad ; \quad h_L = \delta \cdot a_p \quad , \quad \text{(12b; 12c)}$$

and

$$\alpha_L = a\tan\left[\frac{\cos(90-\alpha)}{\sin(90-\alpha)\cos\left[a\tan\left(\frac{b}{2h}\right)\right]}\right] \tag{12d}$$

**dCOP** – Del Carlo, Olujić, Paglianti[28]

Same as Brunazzi and Paglianti (1997), except that instead of film thickness, δ, the product (δ sin $\alpha$) is used in the expression for the Graetz number (Gz)!

**H&C** – Henley, Chen[29]

$$k_L = \frac{D_L}{d_e} 0.33\, \mathrm{Re}_L^1\, Sc_L^{1/3} = \frac{D_L}{d_e} 0.33 \left(\frac{u_{Ls}\rho_L d_e}{\mu_L}\right)\left(\frac{\mu_L}{D_L \rho_L}\right)^{1/3} \tag{13}$$

with

$$d_e = \frac{4\varepsilon}{a_p} \tag{13a}$$

Table 2 – *Geometric features of corrugated sheet structured packings considered in present study*

| | $a_p$ ($m^2\,m^{-3}$) | $b$ (m) | $h$ (m) | $s$ (m) | $\varepsilon$ (–) | $h_{pe}$ (m) |
|---|---|---|---|---|---|---|
| B1–250 | 250 | 0.0226 | 0.0113 | 0.016 | 0.988 | 0.2 |
| B1–500 | 500 | 0.0113 | 0.0057 | 0.008 | 0.975 | 0.2 |

Table 3 – *Physical properties of CB/EB system at different operating pressures as employed in Bayer TS tests (average at middle of the bed temperature)*

| | | |
|---|---|---|
| Pressure, bar | 0.1 | 1.0 |
| Temperature, °C | 67 | 134 |
| Molecular weight, kg kmol$^{-1}$ | 109 | 109 |
| Liquid density, kg m$^{-3}$ | 930 | 870 |
| Liquid viscosity, Pa s | 5.0 E$^{-4}$ | 3.0 E$^{-4}$ |
| Liquid diffusivity, m$^2$ s$^{-1}$ | 3.4 E$^{-9}$ | 6.4 E$^{-9}$ |
| Vapor density, kg m$^{-3}$ | 0.409 | 3.233 |
| Vapor viscosity, Pa s | 8.0 E$^{-6}$ | 10.0 E$^{-6}$ |
| Vapor diffusivity, m$^2$ s$^{-1}$ | 40.0 E$^{-6}$ | 4.2 E$^{-6}$ |
| Vapor phase Schmidt number, – | 0.49 | 0.74 |
| Surface tension, N m$^{-1}$ | 0.025 | 0.020 |
| Relative volatility, – | 1.18 | 1.13 |
| Slope of equilibrium line, – | 0.99 | 1.00 |
| Reference composition (x), – | 0.5 | 0.5 |
| Liquid load, m$^3$ m$^{-2}$ h$^{-1}$, at F-factor = 2 m s$^{-1}$(kg m$^{-3}$)$^{0.5}$ | 4.95 | 14.9 |

the ratio of corrugation side to hydraulic diameter is approximately 1.7, independent of the packing size.

One should note that the RBF correlation is used without the correction term, i.e. $c_E = 1$, which in the original case is $c_E = 0.9$. Therefore, $k_L$ values calculated by the present form adopted in SRP (Separations Research Program) simulation program, Distill 2.0, are somewhat larger than those estimated by the original method, which is in agreement with recent research conducted at SRP.[32] Stripping data used for model validation suggests that the correction factor increases with increasing liquid load to an extent that generates correction factor values above 1. However, dedicated absorption or stripping tests performed with entire resistance concentrated in vapor or liquid phase may not be representative of typical distillation situations.

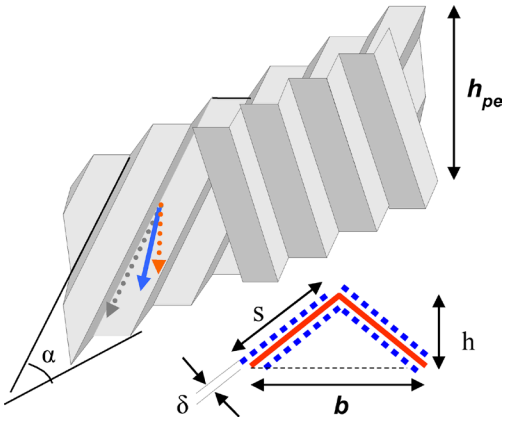


Fig. 1 – *Basic geometry of a corrugated sheet structured packing, with main parameters: (α) corrugation inclination angle, (b) corrugation base, (δ) film thickness, (h) corrugation height, ($h_{pe}$) height of a packing element, and (s) corrugation side. Arrows indicate potential film flow directions*

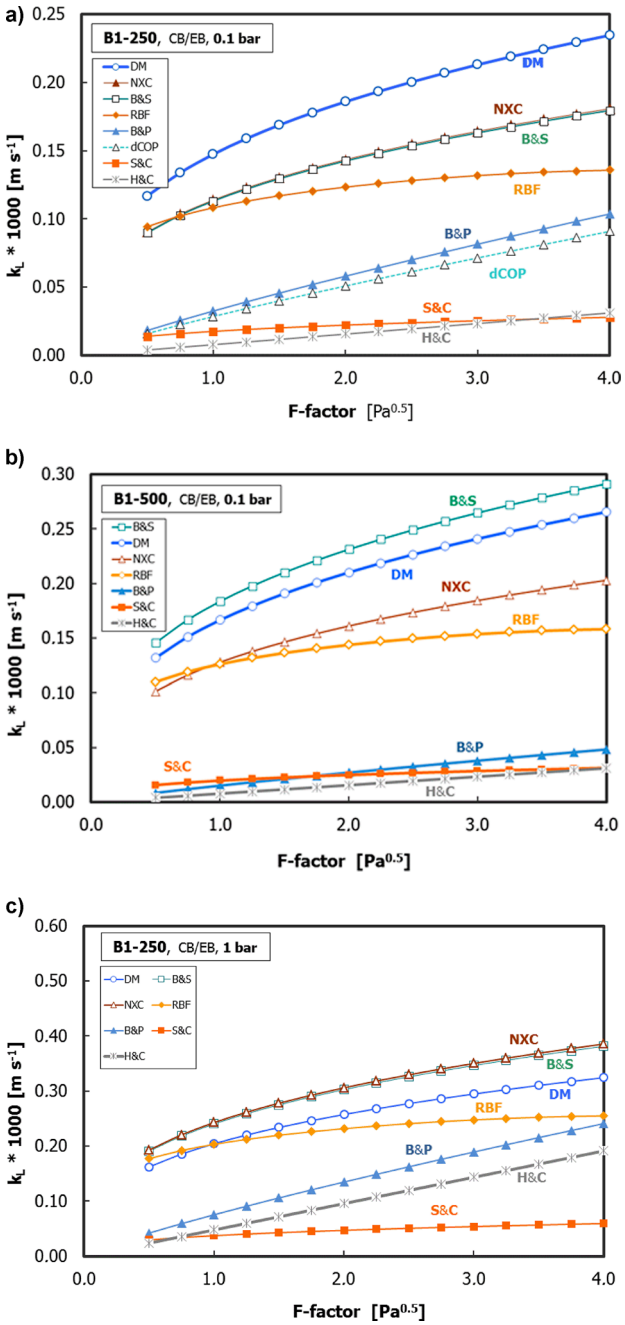


Fig. 2 – *a) Liquid phase mass transfer coefficient as a function of F-factor, as predicted for B1–250 at 0.1 bar; b) Liquid phase mass transfer coefficient as a function of F-factor, as predicted for B1–500 at 0.1 bar; c) Liquid phase mass transfer coefficient as a function of F-factor, as predicted for B1–250 at 1 bar.*

Model comparisons for the 500 m$^2$ m$^{-3}$ packing, shown in Fig. 2b, indicate that doubling the specific packing area leads to a modest increase in $k_L$ values. This is in line with expectations.[32] The relatively much larger increase in the case of the B&S method, on av-

erage around 60 %, is due to the high value of the characteristic coefficient (see Table 1) which was obtained by extrapolation of values published for B1–200 and B1–300 packings.[24] Since the obtained (extrapolated) value ensured good agreement between estimated and measured efficiency, it was considered to be appropriate for the purposes of this study.

Interestingly, the H&C method remains unaffected. This is not surprising since the $k_L$ is proportional to $Re_L$, (exponent of 1 in Eq. 13), which leads to the independence on the hydraulic diameter. Conversely, the B&P method shows an opposite trend similar to that reported by De Britto et al.[19] The decrease in $k_L$ value is rather strong and corresponds closely with the ratio of specific geometric areas. This is a consequence of the B&P $k_L$ method being proportional to the characteristic Graetz number. For example, when compared at an F-factor of 2 $Pa^{0.5}$, a factor 2.4 times larger liquid phase Reynolds number and 1.3 times larger film thickness results in more than three times larger $k_L$ for B1–250 than for B1–500. The issue is caused by the characteristic linear dimension (length scale) being the hydraulic diameter based on the liquid film thickness, a parameter that is "very difficult to quantify" as noted by Weiland et al.[33] All other methods use a characteristic vapor flow channel dimension, which changes proportionally to the change in specific packing area. The dependence of $k_L$ on specific packing area exhibited by the B&P method may be considered incorrect in both trend and value.

As shown in Fig. 2c, similar trends are preserved at 1 bar with absolute values increasing by a factor 1.9 to 2.3, depending on the model which is close to the ratio of liquid diffusivities ($D_{L,0.1\ bar}/D_{L,1\ bar} = 1.9$) at given pressures. An exception is the H&C method, which shows a factor 6 increase. This is a result of the significant dependence of the liquid phase diffusion coefficient with pressure (a factor 1.9 increase) and the direct proportionality of $k_L$ with the Reynolds number (a factor 4.7 increase) in the H&C model. Namely, the liquid viscosity decreases significantly as a result of the higher operating pressure and corresponding temperature. The reduced liquid viscosity leads to an inversely proportional increase in the liquid phase diffusion coefficient. This, together with a small decrease in the liquid density, leads to a factor of 3 decrease in the liquid phase Schmidt number. However, as a result of the low exponent (1/3), such a large reduction in the Schmidt number exhibits a limited compensating effect.

In regards to other discrepancies among compared methods, the highest and lowest predicted values differ on average by a factor of 8 at 1 bar and a factor of 12 at 0.1 bar. Unfortunately, there is no direct experimental evidence available that could serve as a basis for the proper evaluation of accuracy in this respect. The $k_L$ values predicted by theoretically based correlation by Shetti and Cerro[23] are the lowest, by an order of magnitude at 1 bar. The relatively much higher predicted $k_L$ values associated with the DM, B&S and NXK models appear to be less realistic also.

## Vapor phase mass transfer coefficient model prediction comparisons

Figures 3a and 3b show a comparison of predicted vapor phase mass transfer coefficients for

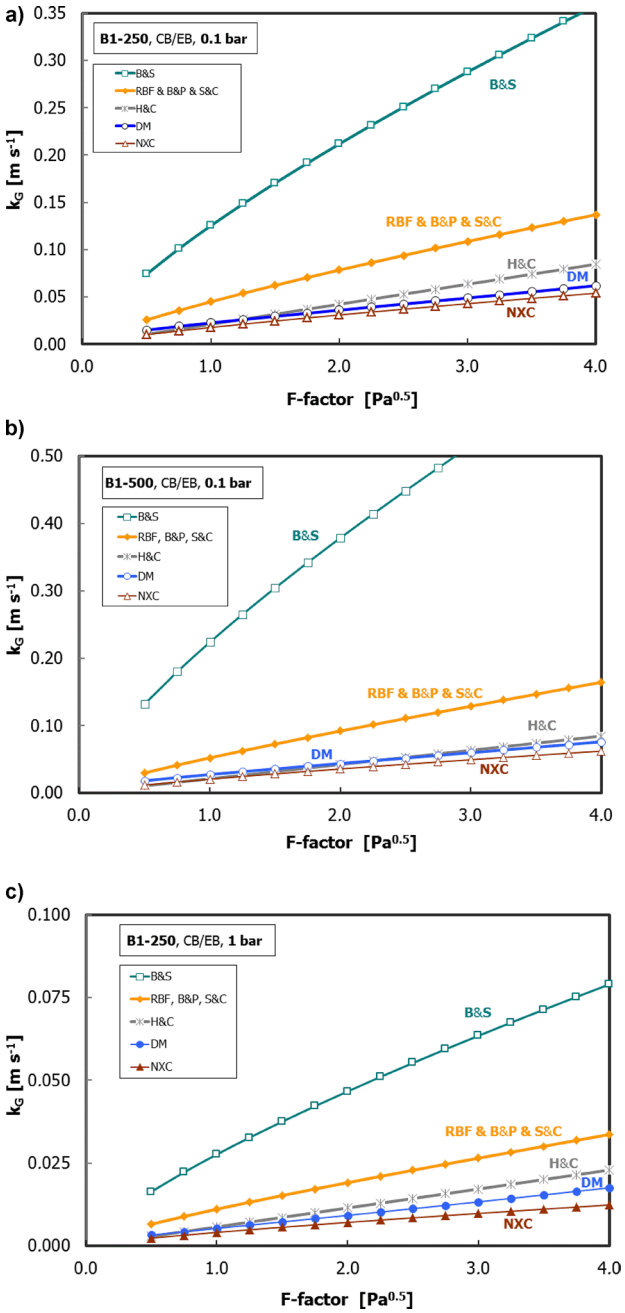


Fig. 3 – *a) Vapor phase mass transfer coefficient as a function of F-factor, as predicted for B1–250 at 0.1 bar; b) Vapor phase mass transfer coefficient as a function of F-factor, as predicted for B1–500 at 0.1 bar; c) Vapor phase mass transfer coefficient as a function of F-factor, as predicted for B1–250 at 1 bar*

B1–250 and B1–500 at 0.1 bar, respectively. As expected, there is an increasing trend with increasing F-factor with the absolute values and steepness of the curve most pronounced in the case of the B&S method. The NXC, DM and H&C methods generate the lowest values, while the values and the slope of the RBF correlation are closer to the DM than to the B&S method. Some methods (B&P and S&C) use the RBF correlation with their own linear dimensions. The model differences are so small that the correlations being compared provide practically equivalent values. It is interesting to note the observed difference between the B&S and other methods to that of the lowest values predicted by NXC. The difference is more than factor of 6 at both pressures using the B1–250 and in the case of B1–500 at 0.1 bar, the difference is factor of 11.

The B&S model showed a pronounced difference (factor 1.8) for the B1–500 packing, which s likely a result of the higher value of the characteristic coefficient obtained by extrapolation for this packing size. Again, an indirect confirmation was found that such a high value ensures a close approach to measured efficiency. For other methods, the doubling of the specific packing area results in a modest increase in the predicted $k_G$, 16 % for RBF and NXC, and 22 % for DM. The exception is again the H&C method, which, as a result of the linear dependence of $k_G$ with $Re_G$, does not observe a packing size related effect.

The pressure effect for B1–250 is demonstrated in Fig. 3c. As a result of a strong dependence of vapor side diffusion coefficient with operating pressure, the corresponding mass transfer coefficients at 0.1 bar are larger by a factor of 4.1 relative to 1 bar, with values ranged from a factor of 3.7 for H&C to 4.5 for B&S method.

As a result of $k_G$ values being much higher than the $k_L$ values, the overall vapor side mass transfer coefficient, $k_{oG}$, exhibits similar behavior. This can be seen from Figs 4a, 4b, and 4c, where $k_{oG}$ curves are shown as a function of F-factor for B1–250 and B1–500 at 0.1 bar and for B1–250 at 1 bar, respectively. Again, the B&S curves exhibit the highest values followed by RBF method. The H&C and NXC methods exhibit the lowest values at 0.1 bar and 1 bar respectively. Similar to the individual vapor phase mass transfer coefficient case, the difference between the highest and lowest predicted values for B1–250 at 1 bar is a factor of 4, and a factor of 6.6 at 0.1 bar. The maximum to minimum difference is a factor of 11.4 for the case of B1–500.

One should note that a factor of 10 decrease in operating pressure (from 1 to 0.1 bar) translates into

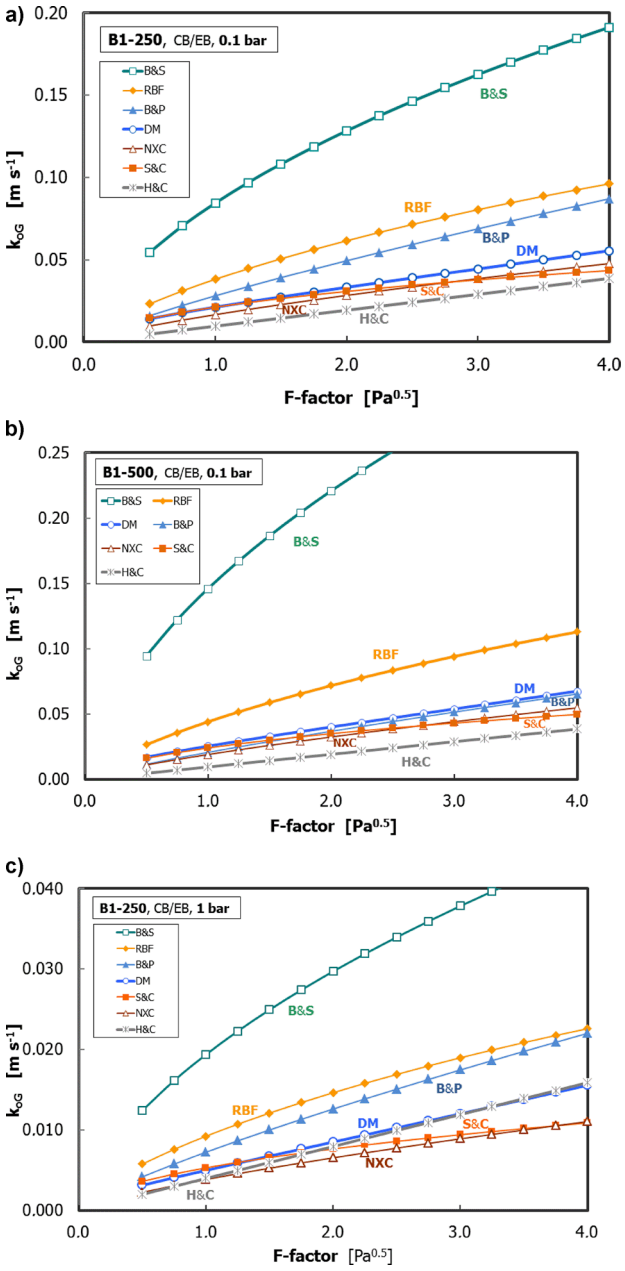


Fig. 4 – *a) Overall vapor phase based mass transfer coefficient as a function of F-factor, as predicted for B1–250 at 0.1 bar; b) Overall vapor phase based mass transfer coefficient as a function of F-factor, as predicted for B1–500 at 0.1 bar; c) Overall vapor phase based mass transfer coefficient as a function of F-factor, as predicted for B1–250 at 1 bar*

approximately four times larger values of $k_{oG}$. This suggests that a much more efficient operation could be expected in vacuum, but experimental evidence (see Pilling and Spiegel[4]; Olujić et al.[30]) indicates no significant pressure effect. This may be the result of a compensating counter-effect. For instance, under vacuum conditions, where low liquid rates prevail, it can be expected that a much lower fraction of installed packing area is used as effective mass transfer area.

## Liquid phase resistance fraction model prediction comparisons

Figures 5a to 5c show the predicted fraction of liquid phase resistance (LRF) to mass transfer as a function of F-factor for B1–250MN at 0.1 bar, B1–500MN at 0.1 bar, and B1–250 at 1 bar, respectively. As reference, constant value lines as predicted by penetration theory assuming equal contact time are shown. Regarding the trend, the fraction of liquid phase resistance should increase with increasing F-factor (or liquid load). This is indeed true with DM, B&S, RBF, NXC and S&C methods. The lowest slope and absolute values are exhibited by DM and NXC methods, while the largest values are predicted by S&C method followed by B&S and RBF methods. As expected, an opposite trend is exhibited by B&P and H&C methods. The observed trends reflect the changes related to the ratios of vapor and liquid mass transfer coefficients.

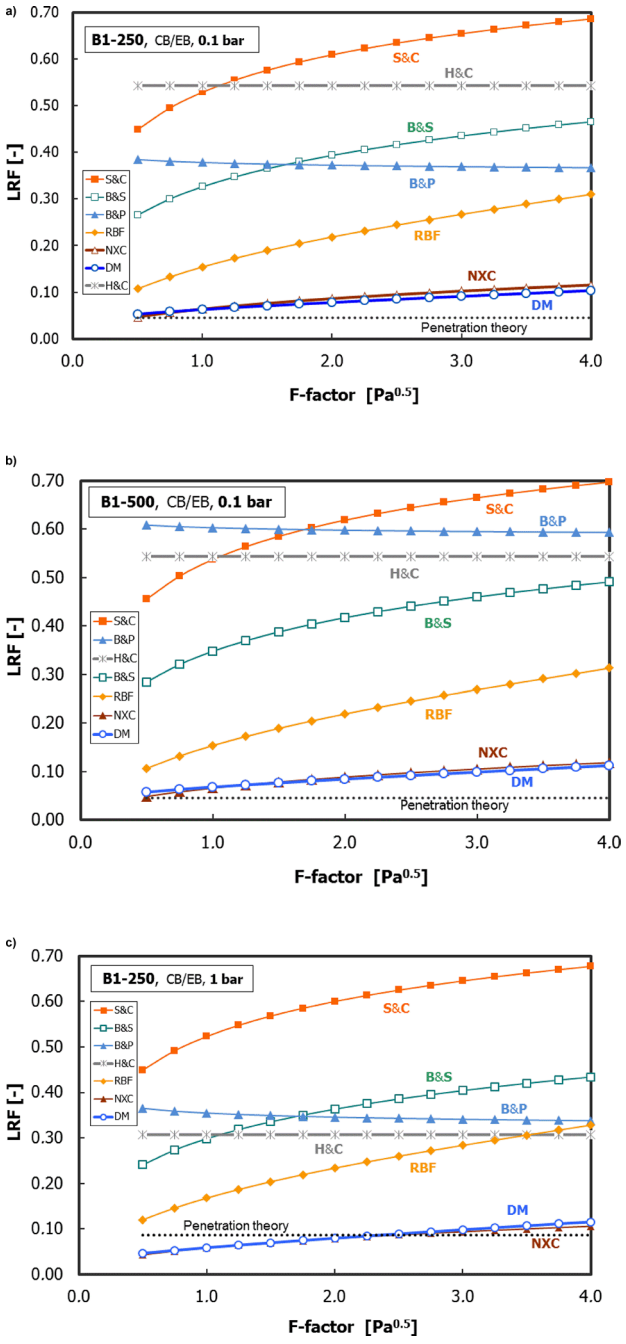


Fig. 5 – *a) Liquid phase resistance fraction as a function of F-factor, as predicted for B1–250 at 0.1 bar; b) Liquid phase resistance fraction as a function of F-factor, as predicted for B1–500 at 0.1 bar; c) Liquid phase resistance fraction as a function of F-factor, as predicted for B1–250 at 1 bar*

At 0.1 bar and an F-factor of 2 $Pa^{0.5}$, the LRF is increasing from 8.7 % predicted by NXC to 61 %, predicted by S&C method, indicating a factor of 7 difference. The LRF predicted by B&P is 37.3 %, which is similar to that of B&S method (39.4 %), while H&C method (54.4 %) approaches S&C method. A similar trend is obtained in the case of B1–500 at 0.1 bar (Fig. 5b) and with B1–250 at 1 bar (Fig. 5c), with the exception of B&P and H&C methods, which exchange places. The deviating behavior of the latter can be attributed to a strong pressure effect, where much lower values of $(k_G/k_L)$ are obtained at 1 bar relative to 0.1 bar (a factor of 20 difference!). In the case of B&P method, the LRF increases significantly with doubling of the specific packing area.

The weakness of H&C method is the direct proportionality between $k_L$ and the $Re_L$, while the B&P absorption based model (with experiments performed with nonvolatile solvents and Mellapak 250.Y packing) used to derive the $k_L$ correlation, could make the model inappropriate for distillation and higher surface area structured packings.

All other methods behave accordingly and appear insensitive to specific geometric area or pressure effect with changes not exceeding 10 %. One should note that the lowest values, estimated by DM and NXC models, approximate values based on penetration theory for both liquid and vapor phase. The fraction of liquid phase resistance is 4.5 % and 8.7 %, respectively, with the square root of the vapor to liquid diffusion coefficient ratio instead of the ratio of mass transfer coefficients, for 0.1 and 1 bar operation.

It is not surprising that B&S method generates highest values since the model relies on film flow theory which assumes a much larger undisturbed liquid flow path and larger contact times. However, the absolute values, some of which are 700 % greater than those based on penetration theory suggest that, depending on the F-factor, approximately 50 to 70 % of the mass transfer resistance is caused by liquid phase which appears too high.

Therefore, it seems reasonable to accept that, in the case of ideal, close boiling systems, such as the ethylbenzene/chlorobenzene mixture, the liquid phase contribution can be significantly larger than

that suggested by penetration theory. This is consistent with the literature suggesting that the fraction of the liquid phase resistance could be significantly larger in distillation than generally believed[14,15] and not limited to non-ideal liquid systems with pronounced variations and high stripping factor values at the bottom of the column. In regards to the well-established correlations, the magnitude of LRF predicted by RBF method (10 – 30 %) appears more realistic than the much higher LRF values predicted by B&S model. The nature and magnitude of potential effects due to modifications in liquid side mass transfer coefficient will be illustrated using the Delft Model.[25,26]

## Delft Model modification considerations

The most distinctive feature of the Delft Model (DM) is that it requires no packing type or size specific empirical coefficient to describe hydraulics and mass transfer performance of both conventional and high capacity/performance corrugated sheet structured packings. Most recent evaluations of the predictive accuracy using total reflux distillation data obtained with various mixtures of primary alcohols[34] and chlorobezene/ethylbenzene[30] indicate that the efficiency predictions are too conservative.

As elaborated in detail elsewhere,[30] the primary cause appears to be a low predicted value of the vapor side mass transfer coefficient (see Figs 3a to 3c) compared to that of established methods. This is a consequence of a decision made in an early stage of model development (Olujić et al.[25]) to effectively reduce the $k_G$ values estimated for turbulent flow mass transfer coefficient by introducing a coefficient that corresponds with the V-shaped fraction of triangular vapor flow channel occupied by liquid ($\varphi \cong 0.6$). This ensures a conservative efficiency prediction, which, in the case of a close boiling system like chlorobenzene/ethylbenzene, is excessive (see Figs. 6 to 8).

As shown in Fig. 6, using $\varphi = 1$, i.e. turbulent vapor phase mass transfer coefficient as generated by original correlation,[35] the DM model generates efficiency predictions for a 250 $m^2$ $m^{-3}$ packing that closely approach the measured efficiency from the safe side. However, in the case of B1–500MN under same operating conditions (0.1 bar), the predicted curve is on the optimistic side (Fig. 7), while at atmospheric pressure, the predicted and observed values agree very well (Fig. 8).

Figures 9 and 10 show predicted (utilizing $k_G$ correlation with $\varphi = 0.6$ in conjunction with original and new $k_L$ correlation, respectively) and measured HETP-curves for cyclohexane/n-hexane system at operating pressures of 0.31 bar and 1.62 bar, respectively, as employed in a recent FRI test with

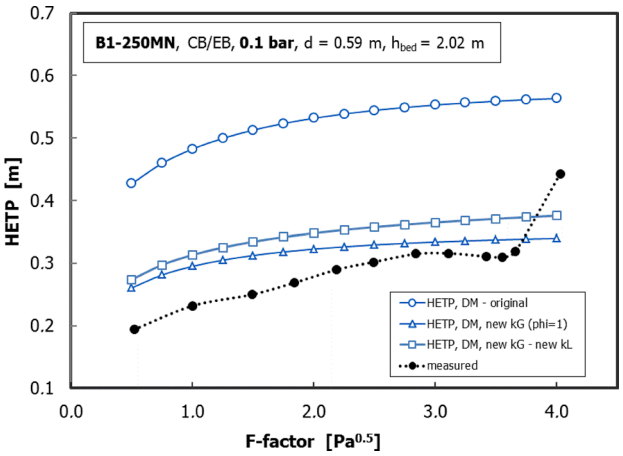


Fig. 6 – *Effect of variation in vapor and liquid phase mass transfer coefficients on predictive accuracy of DM for B1–250 packing at 0.1 bar*

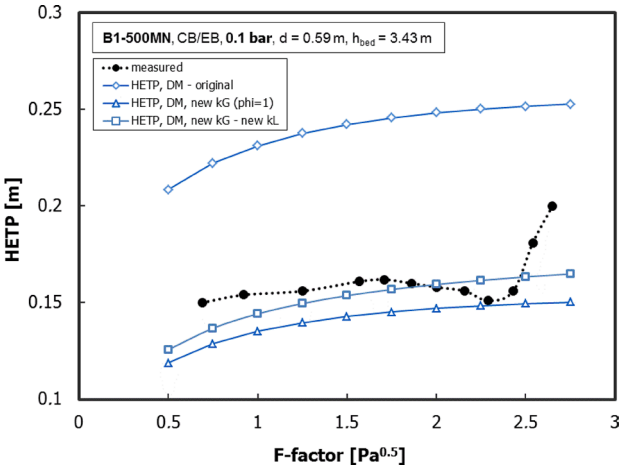


Fig. 7 – *Effect of variation in vapor and liquid phase mass transfer coefficients on predictive accuracy of DM for B1–500 packing at 0.1 bar*

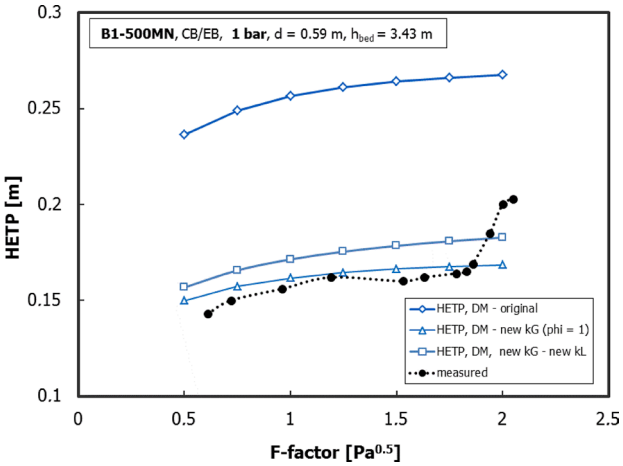


Fig. 8 – *Effect of variation in vapor and liquid phase mass transfer coefficients on predictive accuracy of DM for B1–500 packing at 1 bar*

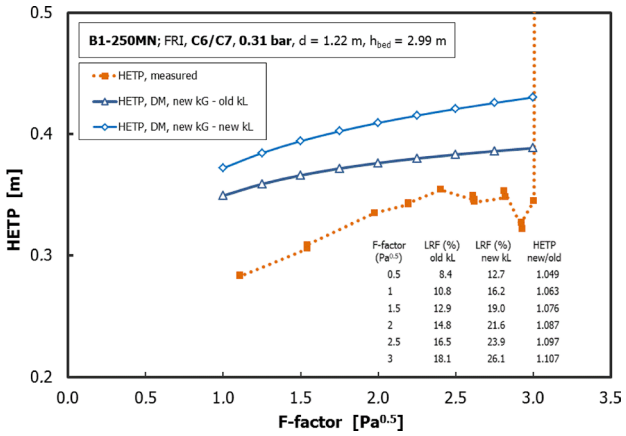


Fig. 9 – *Effect of variation in vapor and liquid phase mass transfer coefficients on predictive accuracy of DM for B1–250 packing at 0.31 bar, for C6/C7 system*[37]

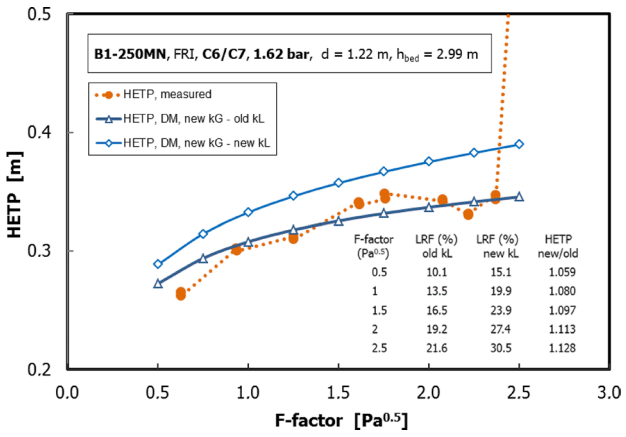


Fig. 10 – *Effect of variation in vapor and liquid phase mass transfer coefficients on predictive accuracy of DM for B1–250 packing at 1.65 bar, for C6/C7 system*[37]

B1–250MN.[36] In both cases, the fraction of liquid side resistance (LRF) increases by approximately a factor of 1.5, inducing an increase in HETP values ranging from 5 % to 10 % at 0.31 bar, and from 6 % to 12 % at 1.62 bar.

It is interesting to mention that the DM method with the new $k_G$ correlation suggests that within the loading region, the amount of liquid side resistance for C6/C7 system is 26 % at 0.31 bar and 31 % at 1.62 bar. This is still somewhat less than predicted by the RBF method. A certain increase in LRF predicted by DM could be obtained by reducing the liquid side mass transfer coefficient values which, as shown in Figs. 1a to 1c, appear to be largest compared to other methods. The DM liquid phase mass transfer coefficient (see Eq. 12 in Table 1) relies on the hydraulic diameter of the triangular flow channel, $d_{hG}$ (m), as the characteristic linear dimension representing penetration theory related liquid film exposure length. This dimension was chosen for practical reasons to have a single triangular channel flow geometry related parameter for all working equations of DM. However, the actual liquid path length is significantly larger and even larger than the corrugation side width, $s$ (m), which is generally considered as the proper parameter in this respect.[21,24]

### *DM liquid phase mass transfer coefficient variation effects*

If the hydraulic diameter of vapor flow channel is replaced by the corrugation side, $s$ (m), then the DM expression for liquid phase mass transfer coefficient translates into Eq. (8) adopted by RBF method.[21] However, using the corrugation side as the contact length may be considered inappropriate. As shown in Fig. 1 and elaborated in detail by Shetty and Cerro[23], a liquid film driven by gravity will flow under an angle steeper than the corrugation angle. Therefore, the effective length of the undisturbed liquid film flow path is significantly longer by an amount depending on the effective liquid flow angle where its length will be equivalent to $s/\sin\alpha_L$. Physically, this assumes the liquid film surface will remain undisturbed while flowing from the upper or outer fold to the lower or inner corrugation fold. On the outer fold there are points of contact with the corrugation ridges of the adjacent sheet oriented in opposite direction. At these points, two crossing liquid flows mix with each other to a certain extent and upon disengagement flow undisturbed to the lower fold. With no physical obstacles in the inner fold, the liquid film continues to flow undisturbed until the outer fold is reached. If potential effects of a regular pattern of holes in the surface of packing are ignored, this effectively extends the flow path length by a factor of two with respect to that covering only one side of the corrugation.

This assumption has been made and adopted in an earlier publication by Spekuljak and Billet.[37] However, there is always a fraction of liquid tending to follow the channel formed by the inner fold. Therefore, the liquid film flowing under a larger angle across the corrugation side mixes with this stream upon reaching the fold. This probably leads to the renewal of surface occurring on both the outer and inner fold, supporting the belief that the effective liquid flow path is equal to the ratio of the corrugation side and the effective liquid flow angle, i.e. $s/\sin(\alpha_L)$ as described by Eq. (12d) in Table 1.

Substituting ($0.9\, d_{hG} \rightarrow s/\sin\alpha_L$) in Eq. 12 yields:

$$k_L = 2\sqrt{\frac{D_L}{\pi}\frac{u_{Le}}{\left(\frac{s}{\sin\alpha_L}\right)}} = 2\sqrt{\frac{D_L}{\pi}\frac{u_{Ls}}{\varepsilon h_L \sin\alpha_L\left(\frac{s}{\sin\alpha_L}\right)}} = 2\sqrt{\frac{D_L}{\pi}\frac{u_{Ls}}{\varepsilon h_L s}} \quad (14)$$

where $u_{Le}$ (m s$^{-1}$) is effective liquid film velocity, $u_{Ls}$ (m s$^{-1}$) is superficial liquid velocity, $\varepsilon$ (-) is packing porosity, and $h_L$ (m$^3$ m$^{-3}$) is the liquid holdup. The latter can be calculated using Eq. (12c) given in Table 1. Regarding the fact that two angles cancel out the effective increase in the liquid velocity may be considered as being caused by reduced bed porosity only.

The original (Eq. 12) and modified DM liquid side mass transfer coefficient correlations (Eq. 14) are compared in Fig 11, including the RBF method for reference. As expected, the DM curves approach that of RBF method but exhibit a somewhat steeper slope. This is caused by a stronger increase in liquid holdup with increasing F-factor which is predicted by the complex correlation employed by the RBF method relative to the DM case. As a result of the DM method assuming complete wetting of the packing surface, the liquid holdup is proportional to the film thickness as described by Eq. 12b which depends on the superficial liquid velocity to an exponent of (1/3).

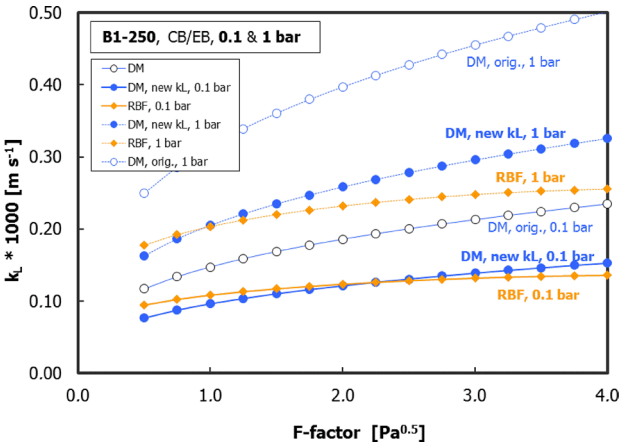


Fig. 11 – *Comparison of $k_L$ value curves predicted by original and new DM correlation as well as RBF correlation, at 0.1 and 1 bar, respectively*

An increased $k_G$ and a decreased $k_L$ have a profound effect on the fraction of the liquid side resistance, as predicted by DM. As shown in Fig. 12, the LRF more than doubles with respect to the original correlation but does not exceed that predicted by RBF. Regarding the absolute values at high vapor loads, both methods suggest a significant contribution of liquid phase to overall mass transfer resistance.

By adopting Eq. (14), the liquid phase resistance predicted by DM will increase, which reduces the predicted efficiency to a certain extent depending on the system. As demonstrated in Figs 6–8 for CB/EB system, this corresponds with a 5 % increase in predicted HETP values compared to that based

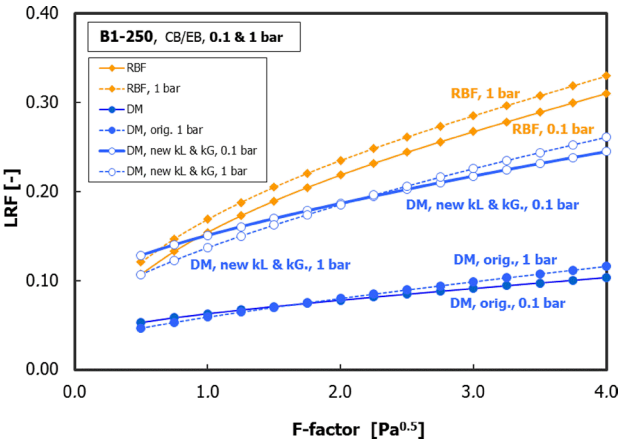


Fig. 12 – *Comparison of LRF value curves predicted by original and new DM correlation as well as RBF correlation, at 0.1 and 1 bar, respectively*

on Eq. (12), which makes predictions for B1–250MN at 0.1 bar and B1–500MN at 1 bar more conservative. The predicted curve for B1–500MN at 0.1 bar now agrees well with the measured values in the loading region. In the case of the C6/C7 system, the increase in predicted HETP values is more pronounced resulting in a more conservative estimate for 0.31 bar (Fig. 9), while at 1.65 bar, the predicted curve is just above the measured curve (Fig. 10). Corresponding values are provided in tables inserted in Figs. 9 and 10, respectively.

## Detailed modeling approaches and experiences

It is important to note the extreme differences between values of liquid and vapor phase mass transfer coefficients predicted by models evaluated in this study. These differences are striking and indicate a worrying insufficiency in our knowledge, and emphasize the need for a better understanding and quantification of distillation mass transfer coefficients of both phases as well as the effective mass transfer area.

Model development should rely on a sound combination of empirical and theoretical considerations. The approaches based on the theory are academically more appealing, especially those involving computational fluid dynamics (CFD).[38–40] Unfortunately, striving for increasing the degree of exactness is not leading to usable models. Nevertheless such papers provide valuable insight into the fluid-dynamics complexities involved with liquid film flow over corrugated sheet structured packing surfaces.

Valuri et al.[38] extended the work of Shetty and Cero,[23] who studied the singly sinusoidal topography, by considering a doubly sinusoidal shape including the effects of the texture frequency and the amplitude on interfacial area. The theoretical model

allows quantification, but the fraction of the packing area that is effectively used appears to be much smaller for large specific surface area packing than predicted by the model.

Luo et al.[39] anticipated insufficient wetting and by combining theoretical considerations and air/water related experiments arrived at a semi-empirical expression describing the width of liquid rivulets which are assumed to be proportional to wetted surface area as a function of governing variables. As expected, the liquid film width tends to increase with increasing liquid load and decreasing corrugation inclination angle, and is generally larger in the case of a textured surface compared to a smooth surface. Also, it appeared that the effect of counter-currently flowing vapor is pronounced at higher flow rates and in the loading region a decrease in liquid film width is predicted though no experimental data supports the decrease.

In a most recent paper, Kohrt et al.[40] present the results of an experimental study designed to determine the effect of surface texturing on the liquid-side mass transfer. They have evaluated unidirectional and bi-directional textures as employed in practice. The mass transfer performance was evaluated in an absorption test with a fully liquid-side controlled mass transfer system with water and different viscosity silicone oils as the liquid phase. As expected, measured $k_L a$ tended to increase with increasing liquid load and was considerably higher for textured than for smooth surfaces with the bi-directional surface being much more effective than the unidirectional one. In all cases, the gas phase appeared to exhibit a limited influence, by enhancing the mass transfer rate by approximately 5 %, and was more pronounced in the case of low than in the case of high viscosity liquids.

However, this as well as other detailed experimental and theoretical studies just confirm what we already know. The results of studies performed using conventional measuring techniques are often used to validate exact models including even those based on CFD. The proposed correlations contain two packings or system related coefficients, while the RBF and DM would require only one correction factor. However, correction factors and packing or system specific constants should be avoided.

Further packing performance characterization, determined from detailed experimental and theoretical considerations, should bring success to the development of robust and practical predictive models. The research efforts at the Berlin Institute of Technology[41] and the University of Toulouse (Raynal and coworkers)[42–44] are both using three-dimensional VOF (volume of fluid) CFD approaches to simulate the actual micro and macro geometry of flow channels.

## Concluding Remarks

Seven predictive methods have been compared with respect to trends and absolute values for predicting the liquid side mass transfer coefficient and the fraction of liquid side resistance using total reflux distillation data for chlorobenzene/ethylbenzene system at two operating pressures, 0.1 and 1 bar. The effects of a factor of ten difference in operating pressure and associated differences in physical properties were evaluated. Since the slope of the equilibrium line for the chlorobenzene/ethylbenzene system is constant and equaled to one, the effects of relative volatility and compositions on the liquid side mass transfer resistance were eliminated from consideration.

A tenfold increase in pressure results in the predicted liquid side mass transfer coefficient values being two to six times greater for 1 bar relative to 0.1 bar, depending on the model. At both pressures, the $k_L$ values increase with increasing F-factor and liquid load. A lower increase in liquid side resistance with F-factor is predicted by theoretically founded S&C method than with the other methods.

Comparison of vapor (gas) side mass transfer coefficients predicted by correlations adopted by different models indicates a much stronger pressure effect as well as a more pronounced difference between maximum and minimum values. The values obtained at 0.1 bar are on average five times greater than the corresponding values at 1 bar, which is in accordance with the effect of pressure on the gas phase diffusion coefficient. The B&S method predicts $k_G$ values that are nearly seven times greater than those of NXC and DM methods. This is also reflected but not as pronounced in the trend and values of the overall gas side based mass transfer coefficient.

In this analysis, the effect of pressure on the fraction of liquid side resistance is insignificant and the majority of the methods (exceptions are the H&C and B&P methods) exhibit an increase in the magnitude of liquid side resistance with increasing F-factor (liquid load). In general, the difference between maximum and minimum values is striking, with a factor of 4 to 5 between B&S method where the liquid side contribution amounts up to 45 %, and the DM method where the maximum value does not exceed 10 %. The RBF method may be considered as an average of these two with values rising from 15 % to 30 %. Similar values are also obtained with the DM method utilizing the new vapor phase and liquid phase mass transfer correlations, which now generate approximately 1.7 times larger values of $k_G$ and 1.3 times smaller $k_L$ values.

The strikingly large differences in absolute values of the predicted liquid phase mass transfer coef-

ficients, also observed with vapor side mass transfer coefficient, suggest that our present knowledge on basic mass transfer phenomena in packed beds is worryingly insufficient.

The present study, using an ideal test system, suggests the presence of a significant amount of liquid phase resistance. These results may indicate that, for the case of non-ideal systems with large stripping factors, the contribution of liquid phase resistance to total resistance may become dominant in the lower half of the stripping section.

Model improvement considerations as demonstrated on the example of DM indicate that there is a need for more consistency in model building. This could eventually be achieved by an in-depth approach to analysis of governing phenomena facilitated with adequate experiments. Unfortunately, it is not possible to arrange total reflux distillation experiments in a way to isolate and quantify directly effective area or individual mass transfer coefficients.

## Nomenclature

$a_e$ – effective (interfacial) area, $m^2\ m^{-3}$
$a_p$ – specific geometric area of packing, $m^2\ m^{-3}$
$b$ – corrugation base length, m
$D_G$ – gas (vapor) phase diffusion coefficient, $m^2\ s^{-1}$
$D_L$ – liquid phase diffusion coefficient, $m^2\ s^{-1}$
$d_{hG}$ – hydraulic diameter for the gas phase, m
$d_e$ – equivalent (hydraulic) diameter, m
$F_G$ – $u_{Gs}(\rho_G)^{0.5}$ – gas load factor, $Pa^{0.5}$ or $m\ s^{-1}\ (kg\ m^{-3})^{0.5}$
$G$ *(or V)* – molar flow rate of the gas (vapor), kmol $s^{-1}$
$Ga_L$ – Galileo number for the liquid, –
$Gz_L$ – Graetz number for the liquid, –
$g$ – gravity acceleration, $m\ s^{-2}$
$HETP$ – height equivalent to a theoretical plate, m
$HTU_G$ – height of a gas (vapor) phase transfer unit, m
$HTU_L$ – height of a liquid phase transfer unit, m
$HTU_{Go}$ – height of an overall gas (vapor) phase related transfer unit, m
$h$ – corrugation height, m
$h_L$ – operating liquid hold up, – ($m^3$ liquid $m^{-3}$ bed)
$h_{pe}$ – height of a packing element, m
$Ka_L$ – Kapitsa number for the liquid, –
$k_G$ – vapor phase mass transfer coefficient, $m\ s^{-1}$
$k_{Go}$ – overall vapor phase based mass transfer coefficient, $m\ s^{-1}$
$k_L$ – liquid phase mass transfer coefficient, $m\ s^{-1}$
$L$ – molar flow rate of the liquid, kmol $s^{-1}$
$M_{wG}$ – molar mass of the vapor, $kg\ kmol^{-1}$
$M_{wL}$ – molar mass of the liquid, $kg\ kmol^{-1}$
$m$ – slope of the equilibrium line, –
$NTU_{Go}$ – overall number of vapor phase transfer units
$Re_L$ – Reynolds number for the liquid, –
$Sc_L$ – Schmidt number for the liquid, –
$s$ – corrugation side length, m
$u_{Ge}$ – effective gas (vapor) velocity, $m\ s^{-1}$
$u_{Gs}$ – superficial gas (vapor) velocity, $m\ s^{-1}$
$u_{Le}$ – effective liquid velocity, $m\ s^{-1}$
$u_{Ls}$ – superficial liquid velocity, $m\ s^{-1}$
$We_L$ – Weber number for the liquid, –
y – mole fraction of more volatile component in vapor, –
x – mole fraction of more volatile component in liquid, –

## Greek letters

$\alpha$ – corrugation inclination angle, with respect to horizontal axis, °
$\alpha_L$ – effective liquid flow angle, °
$\alpha$ – relative volatility of the light component, –
$\delta$ – liquid film thickness, m
$\varepsilon$ – packing porosity, $m^3$ voids $m^{-3}$ bed
$\varphi$ – fraction of the triangular flow channel occupied by liquid, –
$\lambda$ – m/(L/G) – stripping factor, –
$\rho_G$ – density of the gas (vapor), $kg\ m^{-3}$
$\rho_L$ – density of the liquid, $kg\ m^{-3}$
$\sigma$ – surface tension, $N\ m^{-1}$

## Subscripts

$G$ – gas or vapor
$L$ – liquid

## References

1. *Olujić, Ž., Jödecke, M., Shilkin, A., Schuch, G., Kaibel, B.*, Equipment improvement trends in distillation, Chem. Eng. Process. **48** (2009) 1089. http://dx.doi.org/10.1016/j.cep.2009.03.004
2. *Olujić, Ž.*, Packed columns: High capacity internals, under II/Distillation, in: I. D. Wilson, C. F. Poole, M. Cooke (Eds), Encyclopedia of Separation Sciences, Online Update 1, Elsevier, 2007. http://dx.doi.org/10.1016/B978–012226770–3/10670–3
3. *Olujić, Ž., Seibert, A. F., Kaibel, B., Jansen, H., Rietfort, T., Zich, E.*, Performance characteristics of a new high capacity structured packing, Chem. Eng. Process. **42** (2003) 55. http://dx.doi.org/10.1016/S0255–2701(02)00019–3
4. *Pilling, M., Spiegel, L.,* Design characteristics and test validation of high performance structured packing, Separations Technology Topical Symposium, AIChE Annual Meeting, November 4–9, 2001, Reno, NV, USA, Vol. 1, 64.
5. *Tsai, R. E., Seibert, A. F., Eldridge, R. B. and G. T. Rochelle*, A dimensionless model for predicting the mass transfer area of structured packing, AIChE J., **57** (2011) 1173. http://dx.doi.org/10.1002/aic.12345
6. *Stichlmair, J. G., Fair, J. R.*, Distillation – Principles and Practice, Wiley-VCH, 1998, pp 395–462.

7. *Harriott, P.*, The effect of liquid-phase resistance on the efficiency of distillation plates, Ind. Eng. Chem. Res. **44** (2005) 5298. http://dx.doi.org/10.1021/ie040240d
8. *Johnstone, H. F., Pigford, R. L.*, Distillation in a wetted wall column, Trans. AIChE **37** (1941) 25.
9. *Kayihan, F., Sandall, O. C., Mellichamp, D.,* Simultaneous heat and mass transfer in binary distillation-I, Chem. Eng. Sci. **30** (1975) 1333. http://dx.doi.org/10.1016/0009–2509(75)85062–7
10. *Kayihan, F., Sandall, O. C., Mellichamp, D.*, Simultaneous heat and mass transfer in binary distillation-II, Chem. Eng. Sci. **32** (1977) 747. http://dx.doi.org/10.1016/0009–2509(77)80124–3
11. *Arwikar, K. J., Sandall, O. C.,* Liquid phase mass transfer resistance in a small scale packed distillation column, Chem. Eng. Sci. **35** (1980) 2337. http://dx.doi.org/10.1016/0009–2509(80)87012–6
12. *Bennett, D. L.*, Optimize distillation columns, Part II: Packed columns, Chem. Eng. Progress **96** (2000) 5, 27.
13. *Wang, G. Q., Yuan, X. G., Tang, Z. L., Chen, J. B., Yu, K. T.*, A short-cut method for estimating the HETP of structured packing distillation columns at elevated pressure, Chem. Eng. Technol. **28** (2005) 767. http://dx.doi.org/10.1002/ceat.200500065
14. *Chen, G. X., Chuang, K. T.,* Liquid-phase resistance to mass transfer on distillation trays, Ind. Eng. Chem. Res. **34** (1995) 3078. http://dx.doi.org/10.1021/ie00048a019
15. *Rejl, F. J., Valenz, L., Linek, V.*, "Profile method" for the measurement of $k_L a$ and $k_V a$ in distillation columns. Validation of rate-based distillation models using concentration profiles measured along the column, Ind. Eng. Chem. Res. **49** (2010) 4383. http://dx.doi.org/10.1021/ie901690m
16. *Wang, G. Q., Yuan, X. G., Yu, K. T.,* Review of mass-transfer correlations for packed columns, Ind. Eng. Chem. Res. **44** (2005) 8715. http://dx.doi.org/10.1021/ie050017w
17. *Bravo, J. L., Rocha, J. A., Fair, J. R.*, Pressure drop in structured packings, Hydrocarbon Processing **64** (1985) 1, 91.
18. *Nawrocki, P. A., Xu, Z. P., Chuang, K. T.,* Mass transfer in structured corrugated packing, Can. J. Chem. Eng. **69** (1991) 1336. http://dx.doi.org/10.1002/cjce.5450690614
19. *De Britto, M. H., von Stockar, U., Bomio, P.,* Predicting the liquid phase mass transfer coefficient – $k_L$ – for the Sulzer structured packing Mellapak, IChemE Symp. Series **128** (1992) B137.
20. *Hanley, B., Dunbobbin, B., Bennett, D.,* A unified model for countercurrent vapor/liquid packed columns. 2. Equations for the mass-transfer coefficients, mass-transfer area, the HETP, and the dynamic holdup, Ind. Eng. Chem. Res. **33** (1994) 1222. http://dx.doi.org/10.1021/ie00029a018
21. *Rocha, J. A., Bravo, J. L., Fair, J. R.,* Distillation columns containing structured packings: A comprehensive model for their performance. 2. Mass-transfer model, Ind. Eng. Chem. Res. **35** (1996) 1660. http://dx.doi.org/10.1021/ie940406i
22. *Brunazzi, E., Paglianti, A.,* Liquid film mass-transfer coefficient in a column equipped with structured packings, Ind. Eng. Chem. Res. **36** (1997) 3792. http://dx.doi.org/10.1021/ie970045h
23. *Shetty, S., Cerro, R.*, Fundamental liquid flow correlations for the computation of design parameters for ordered packings, Ind. Eng. Chem. Res. **36** (1997) 771. http://dx.doi.org/10.1021/ie960627j
24. *Billet, R., Schultes, M.,* Prediction of mass transfer columns with dumped and arranged packings. Updated summary of the calculation method of Billet and Schultes, Chem. Eng. Res. Des. **77** (1999) 498. http://dx.doi.org/10.1205/026387699526520
25. *Olujić, Ž., Kamerbeek, A. B., de Graauw, J.,* Corrugation geometry based model for efficiency of structured distillation packings, *J*., Chem. Eng. Process. **38** (1999) 683. http://dx.doi.org/10.1016/S0255–2701(99)00068–9
26. *Olujić, Ž., Behrens, M., Colli, L., Paglianti, A.,* Predicting the efficiency of corrugated sheet structured packings with large specific geometric area, Chem. Biochem. Eng. Q. **18** (2004) 89. http://dx.doi.org/10.1016/S1369–703X(03)00170–0
27. *Xu, Z. P., Afacan, A., Chuang, K. T.*, Predicting mass transfer in packed columns containing structured packings, Chem. Eng. Res. Des. **78** (2000) 91. http://dx.doi.org/10.1205/026387600526924
28. *Del Carlo, L., Olujić, Ž., Paglianti, A*., Comprehensive mass transfer model for distillation columns equipped with structured packings, Ind. Eng. Chem. Res. **45** (2006) 7967. http://dx.doi.org/10.1021/ie060503z
29. *Hanley, B., Chen, C.-C.,* New Mass-transfer correlations for packed towers, AIChE J. **58** (2012) 132. http://dx.doi.org/10.1002/aic.12574
30. *Olujić, Ž., Rietfort, T., Jansen, H., Kaibel, B., Zich, E., Frey, G., Ruffert, G., Zielke, T.,* Experimental characterization and modelling of high performance structured packings, Ind. Eng. Chem. Res. **51** (2012) 4414. http://dx.doi.org/10.1021/ie202585t
31. *Ottenbacher, M., Olujić, Ž., Adrian, T., Jödecke, M., Großmann, C.*, Structured packing efficiency – Vital information for the chemical industry, Chem. Eng. Res. Des. **89** (2011) 1427.
32. *Murrieta, C. R., Seibert, A. F., Fair, J. R., Rocha, J. A.,* Liquid-side mass-transfer resistance of structured packings, Ind. Eng. Chem. Res. **43** (2004) 7113. http://dx.doi.org/10.1021/ie049836r
33. *Weiland, R. H., Ahlgren, K. R., Evans, M.*, Mass-transfer characteristics of some structured packings, Ind. Eng. Chem. Res. **32** (1993) 1411. http://dx.doi.org/10.1021/ie00019a015
34. *Valenz, L., Rejl, F. J., Linek, V., Olujić, Ž.,* Experimental evaluation of the mass transfer models for predicting the efficiency of structured packings, CD Rom Proceedings, CHISA 2010 – ECCE 7, 28 August – 1 September 2010, Prague, Czech Republic.
35. *Olujić, Ž.,* Development of a complete simulation model for predicting the hydraulic and separation performance of distillation columns equipped with structured packings, Chem. Biochem. Eng. Q. **11** (1997) 31.
36. *Olujić, Ž., Kaibel, B., Rietfort, T., Jansen, H., Zich, E.*, Fractionation Research Inc. test data and modelling of a high-performance structured packing, Ind. Eng. Chem. Res. **52** (2013) 4888. http://dx.doi.org/10.1021/ie302715x
37. *Spekuljak, Z., Billet, R.,* Mass transfer in regular packing, Lat. Am. J. Heat Mass Transfer **11** (1987) 63.
38. *Valuri, P., Matar, O. K., Hewitt, G. F., Mendes, M. A.,* Thin film flow over structured packings at moderate Reynolds numbers, Chem. Eng. Sci. **60** (2005) 1965. http://dx.doi.org/10.1016/j.ces.2004.12.008

39. *Luo, S., Li, H., Fei, W., Wang, Y.*, Liquid film characteristics on surface of structured packing, Chinese J. Chem. Eng. **17** (2009) 47. http://dx.doi.org/10.1016/S1004–9541(09)60031–8
40. *Kohrt, M., Ausner, I., Wozny, G. Repke, J.-U.,* Texture influence on liquid side mass transfer, Chem. Eng. Res. Des. **89** (2011) 1410. http://dx.doi.org/10.1016/j.cherd.2011.01.010
41. *Subramanian, K., Wozny, G.,* Analysis of hydrodynamics of fluid flow on corrugated sheets of packings, Int. J. Chem. Eng., Volume 2012 (2012), 13 pages (open access) http://dx.doi.org/10.1155/2012/838965
42. *Raynal, L., Ben-Rayana, F., Royon-Lebeaud, A.*, Use of CFD for $CO_2$ absorbers optimum design: from local scale to large industrial scale, Energy Procedia 1 (2009) 917. http://dx.doi.org/10.1016/j.egypro.2009.01.122
43. *Haroun, Y., Raynal, L., Legendre, D.,* Mass transfer and liquid holdup determination in structured packing by CFD, Chem. Eng. Sci. **75** (2012) 342. http://dx.doi.org/10.1016/j.ces.2012.03.011
44. *Haroun, Y., Raynal, L., Alix, P.,* Prediction of effective area and liquid holdup in structured packings by CFD, Chem. Eng. Res. Des. 92 (2014) 2247. http://dx.doi.org/10.1016/j.cherd.2013.12.029.